

# EFFECTS OF POLYMER STRUCTURE ON THE ELECTROSPUN POLYAMIDE NANOFIBERS

## POLİMER YAPISININ ELEKTROÇEKİMLİ POLAMİD LİFLERİ ÜZERİNE ETKİSİ

Aylin KAYA<sup>1</sup>, Aslı HOCKENBERGER<sup>2</sup>

<sup>1</sup>TUBITAK Bursa Test and Analysis Laboratory, Bursa, TURKEY

<sup>2</sup>Uludag University, Department of Textile Engineering, Bursa, TURKEY

Received: 03.01.2017

Accepted: 01.10.2017

### ÖZET

Bu çalışmanın amacı, farklı molekül yapılarının elektroçekimli poliamid nanolifler üzerine etkisinin incelenmesidir. Poliamid 6 ile poliamid 6.6, konvansiyonel tekstil ürünlerinde yaygın olarak kullanılırken poliamid 4.6, mühendislik uygulamalarına uygun benzersiz özelliklere sahip bir polimerdir. Poliamid cipsleri formik asitte çözülmüş ve tek iğneli elektroçekim makinesi kullanılarak farklı konsantrasyonlarda çekim yapılmıştır. Elde edilen nanoliflerin yüzey özellikleri taramalı elektron mikroskopunda incelenmiş ve lif çapları ölçülmüştür. Isıl özellikler ise DSC ile belirlenmiştir. Yüzey gerilimi ve mekanik özellikler test edilmiştir. Çalışmada elde edilen veriler; nano ölçekte bu üç polimerin lif çapı, kopma mukavemeti, yüzey gerilimi ve ısıl karakterlerin karşılaştırılması için kullanılmıştır. Sonuç olarak poliamid 4.6'nın incelenen polimerler arasında nanolif üretme açısından en iyi yapı ve kristalinite değerlerine sahip poliamid olduğu tespit edilmiştir.

**Keywords:** Poliamid, elektroçekim, nanolif, SEM, DSC

### ABSTRACT

The aim of this research is to investigate the effects of different molecular structures on the polyamide electrospun nanofibers. Polyamide 6, polyamide 6.6 are widely used in conventional textiles and polyamide 4.6 is a unique polymer for its properties suitable for engineering applications. Polyamide pellets were dissolved in formic acid and electrospun in different concentrations using a single nozzle electrospinning machine. The surface properties of these nanofibers were inspected in SEM and fiber diameters were measured. Thermal inspections were conducted using DSC. Surface tension and mechanical properties were also investigated. The data obtained from the study were compared to evaluate the changes in the fiber diameter, tensile strength, surface tension and thermal characterization of these three polymers in nano scale. As a result, it was concluded that Polyamide 4.6 had the most superior structural and crystallinity properties to produce nanofibers among the three polyamides investigated.

**Anahtar Kelimeler:** Polyamide, electrospinning, nanofiber, SEM, DSC

**Corresponding Author:** Aylin Kaya, aylin.celikbilek@tubitak.gov.tr

### 1. INTRODUCTION

Fiber diameter is one of the most crucial factors on the performance and quality of conventional and technical textiles. Despite natural fibers, regenerated and synthetic fibers are suitable for tailoring the fiber properties thus the final product. Different conventional spinning techniques (dry, melt, gel, wet) enables the production of micron and even sub-micron sized fibers. Almost known for more than 80 years, electrospinning is an efficient technique for producing fibers ranging from several microns down to fibers with diameter lower than 100 nm. Nanofibers are

produced by the application of a high voltage to polymer melt or solution in a capillary or tube with a pipette or needle as shown in Figure 1. An electrode which is connected to the high voltage is immersed into the polymer fluid in the capillary or connected to the tip of the nozzle. Another electrode is connected to a stable or rotating metal collector which is facing the nozzle from a specific distance. The solution is held by the surface tension in the form of a droplet when no power is supplied. When the voltage is applied between the electrodes, an electric field becomes dominant on the polymer solution and as the intensity of the

electric field increases, the surface tension of the polymer fluid becomes weaker and the highly charged polymeric fluid forms a conical droplet called Taylor cone. At a specific voltage, the droplet elongates and after the critical point, a single electrically charged jet ejects from the apex of the Taylor cone and travels to the opposite charged electrode that is attached to the collector. As the jet travels, the solvent in the polymeric fluid evaporates (or cools in the case of melt electrospinning) thus the jet solidifies while reaching the collector.

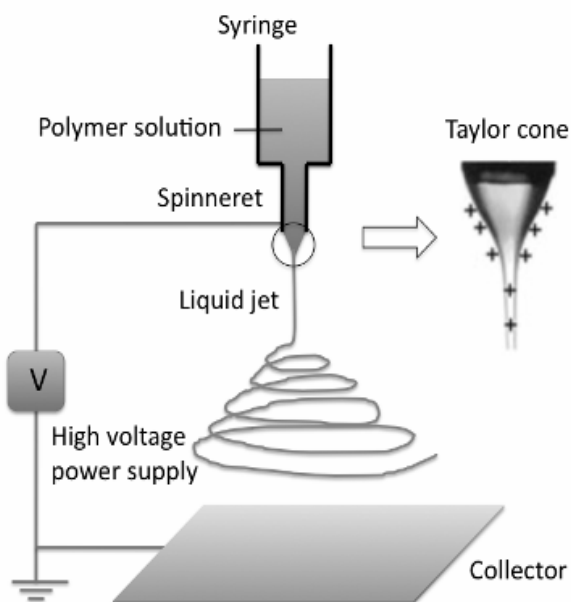


Fig.1. The schematic of electrospinning process (1)

The structure of the nanofibrous surfaces is effected by: (a) Polymer fluid variables (polymer type, molecular weight, solvent type, vapour pressure, diffusivity in air, additives, surfactants, salts, polymer concentration, viscosity, electric conductivity, dielectric permittivity, surface tension etc.), (b) Process variables (solution feed rate, electric potential at the capillary tip, distance between the tip and the collector, nozzle orifice diameter, electric field strength and geometry) and (c) ambient parameters (temperature, humidity, air velocity in the electrospinning chamber etc.) (2,12). A broad review of electrospinning studies could be found in literature cited (3).

Among aliphatic polyamides that are commercially well-known, polyamide 6 and polyamide 6.6 were chosen in this research as they form 90% of polyamide production worldwide (4).

Polyamide 4.6 was preferred as the third polyamide type because of its high mechanical performance, good dimensional stability as well as toughness and stiffness especially favourable in automotive industry. The main reason for this superior performance is the high number of amide units in the main molecule chain, which gives the molecule a higher percentage of crystallinity and enhances the formation of hydrogen bonds (14). The chemical structures of PA 6, PA 6.6 and PA 4.6 were given in Figure 2.

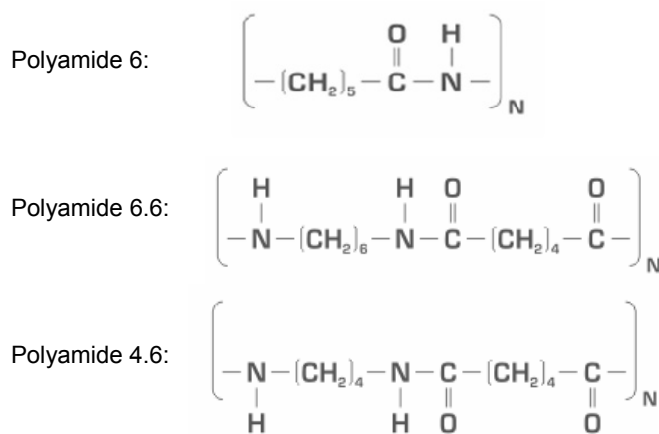


Fig.2. The chemical structures of PA6, PA 6.6 and PA 4.6

Polyamides generally have high abrasion resistance, low friction coefficient, good resilience, high impact resistance and chemical resistance. Polyamide's tendency to binding water (nearly 8.5%) is high due to the hydrogen bonding characteristics of the amide groups (-CONH) present in its structure. As the amide group concentration gets lower in the polymer chain, water absorption gets lower as well (For exp. polyamide 11 has 1,9% water absorption rate where polyamide 6.6 has 9%) (5). Polyamide types differ in their CH<sub>2</sub>/CONH group ratios, giving each of them different molecular properties of crystallinity and -OH linkages. In literature there are many studies investigating the influence of various parameters on the electrospinning of many natural and synthetic polymers. In this study, the effect of variations in the polymeric structure of polyamides on the thermal and mechanical properties of resulting nanofibers were investigated. Three leading polyamide types: polyamide 6, polyamide 6.6 and polyamide 4.6 were electrospun in three different concentrations using formic acid as solvent. The resulting nanofibrous surfaces were analysed using scanning electron microscope for surface investigation and fiber diameter measurement, DSC for determination of melting temperature and crystallinity. Surface angle measurement and tensile testing were also applied to the samples. The results obtained were compared in the view of polymeric structural differences.

## 2. MATERIAL and METHOD

### 2.1. Materials

Polyamides provided from textile and automotive industrial suppliers have the properties given in Table 1.

### 2.2. Methods

#### 2.2.1. Polymer solution preparation and electrospinning

Three different concentrations in all polyamides were prepared using magnetic stirrer: 13%, 16% and 20% (w/v). These concentrations were chosen on the basis of pre-studies and were found to be the most suitable values for both dissolving and processing (above 20% concentration, pellets did not dissolve completely without heating and below 13%, electrospinning was not successful as the

concentration was very low to obtain homogeneous and continuous nanofibers). Ref. [8] and [13] provide information on solvent and polymer interactions effecting electrospinning.

The viscosity of the solutions were measured using a rotational viscometer HOOKE 7Plus Model: 3220 model, at 23°C.

Electrospinning was performed on KATO Tech Model 2080202 NEU-N using a 21 gauge needle. The fibers produced were collected on a rotational cylinder with a 10 cm diameter having 31,54 cm/min traverse speed. Electrospinning conditions were given in Table 2.

### 2.2.2. Characterisation

The nanofibrous samples were dried at room temperature after the electrospinning and tensile testing of the samples

were conducted using TESTOMETRIC M350 -10CT with a load cell of 5 kg. For tensile testing, average of 15 measurements of 5mm\*10 mm cut samples were taken in 23°C, 50% RH conditions.

The surface structure and fiber diameter measurements of the samples were studied using a TESCAN VEGA 3 model scanning electron microscope. To determine the fiber diameter, 50 measurements were done and arithmetic mean was calculated.

For determination of  $T_m$ , heat of fusion ( $H_f$ ) and related crystallisation rate of every sample, Perkin Elmer Sapphire model DSC was used with an increment of 10 °C/min up to 330°C.

Surface tension of the samples were measured via contact angle measurements in a PC controlled surface angle measurement device.

**Table 1.** Properties of polyamide pellets used in the electrospinning.

Polymer Type	Molecular Weight (Dalton)	Glass Temperature ( $T_g$ )	Melting Temperature ( $T_m$ )	Crystallinity (%)
PA 6	32.788	58	225	26,1
PA 6.6	41.063	67	264	26,1
PA 4.6	65.514	-	293	89,4

The polyamide pellets were dissolved in formic acid in 98% purity with the Merck no. 100264.

**Table 2.** Electrospinning process conditions

Polymer	Concentration (%)	Viscosity (mPaS)	Feeding Rate (ml/h)	Applied voltage (kV)	Speed (m/min)
PA6	13	120	0,47	18,7	10,04
	16	175	0,44	19,1	10,04
	20	485	0,51	20,9	10,04
PA 6.6	13	165	0,61	24,9	10,04
	16	255	0,73	23	10,04
	20	770	0,61	21,8	10,04
PA 4.6	13	425	0,51	20	10,04
	16	540	0,73	20	10,04
	20	1900	0,49	20	10,04

### 3. RESULTS and DISCUSSION

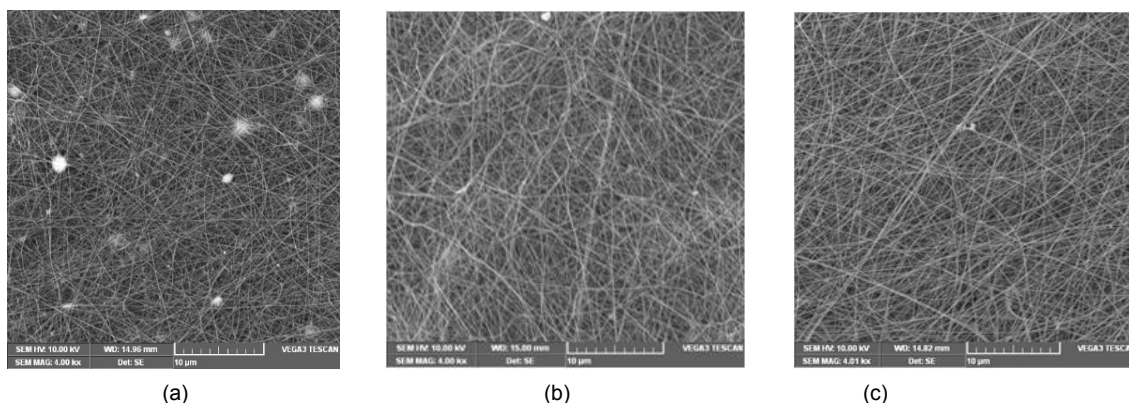


**Fig.3.** The SEM photos of polyamide 6 electrospun nanofibers of concentrations 13% (a), 16% (b) and 20% (c) in ca.4000x (1)

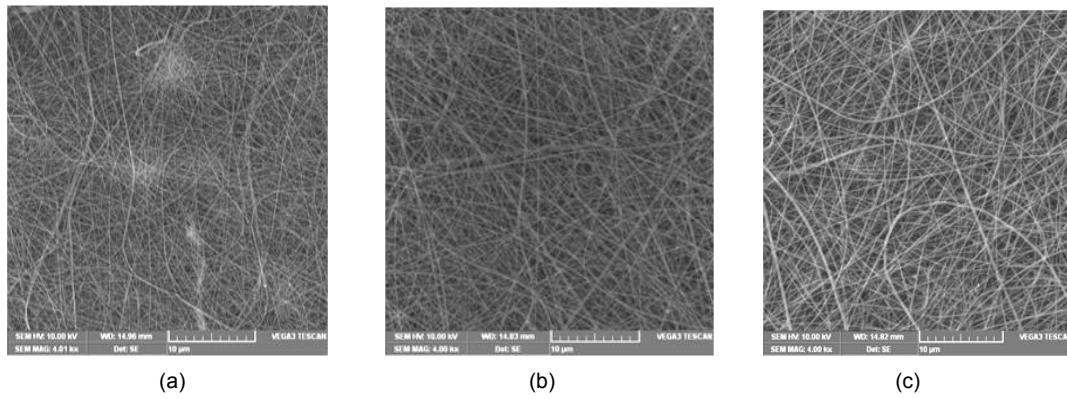


**Fig.4.** The SEM photos of polyamide 6.6 electrospun nanofibers of concentrations 13% (a), 16% (b) and 20% (c) in ca.4000x (1)

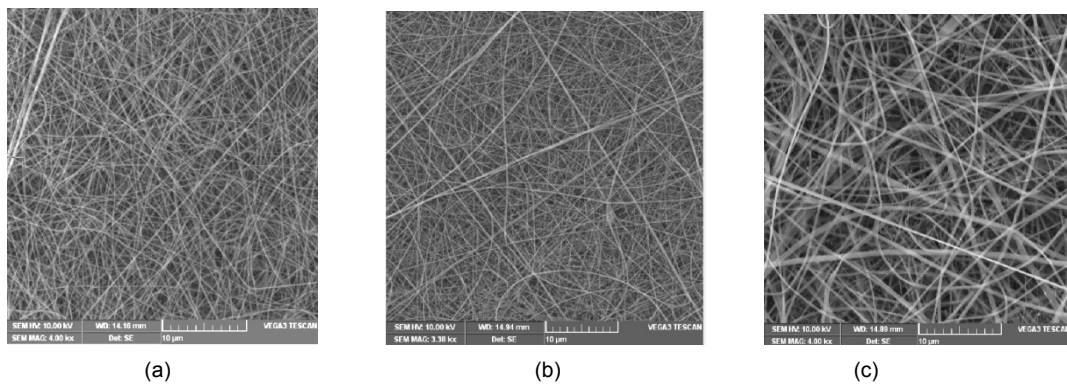


**Fig.5.** The SEM photos of polyamide 4.6 electrospun nanofibers of concentrations 13% (a), 16% (b) and 20% (c) in ca.4000x (1)

**Table 3.** Mean fiber diameter of polyamide nanofibrous surfaces

Polymer	Concentration (%)	Mean fiber diameter (nm)	Standard Deviation	CV %
PA6	13	105,54	23,01	21,8
	16	125,92	26,11	20,73
	20	149,81	33,54	22,39
PA 6.6	13	128,60	21,52	16,73
	16	182,44	30,46	16,70
	20	241,37	48,41	20,06
PA 4.6	13	152,28	15,22	10,00
	16	185,54	48,05	25,90
	20	313,29	60,53	19,32

Electrospun surfaces were examined using scanning electron microscope (Figure 3, 4, 5) and for polyamide 6, it was observed that polymer concentration of 13% resulted in fiber diameters as low as 100 nm and below despite bead formation (Figure 3-a, Table 3). Concentrations of 16% and 20% PA 6 resulted in bead-free nanofibers around 125-150 nm fiber diameter (Figure 3-b, 3-c, Table 3). PA 6.6 had some irregular fiber diameter regions (Figure 4-a) due to the low amount of polymer in 13% concentration but this is comparatively lower than PA 6 of the same concentration thus resulting a more homogenous surface and fiber diameters around 128 nm (Table 3). Fiber diameters rose above 200 nm and smooth nanofibrous surface was

obtained in 20% concentration (Figure 4-c, Table 3). PA 4.6 was the most viscous polymer solution amongst all polyamides and it was electrospun without any surface irregularities even in 13% concentration (Figure 5-a) and fiber diameters were higher than the other polymer types especially in 20% concentration (Table 3).

Surface contact angle measurements, given in Table 4, showed that all polymers showed good wetting properties due to lower contact angles; especially in PA 4.6, remained stable around 60° regardless of the concentration changes-probably due to high molecular weight and symmetry of the molecule chain- but in PA 6 and 6.6 showed variations in different concentrations.

**Table 4.** Mean surface contact angle of polyamide nanofibrous surfaces

Polymer	Concentration (%)	Surface Contact Angle (°)
PA6	13	65,556
	16	70,448
	20	53,165
PA 6.6	13	64,462
	16	41,570
	20	73,454
PA 4.6	13	59,200
	16	63,027
	20	61,982

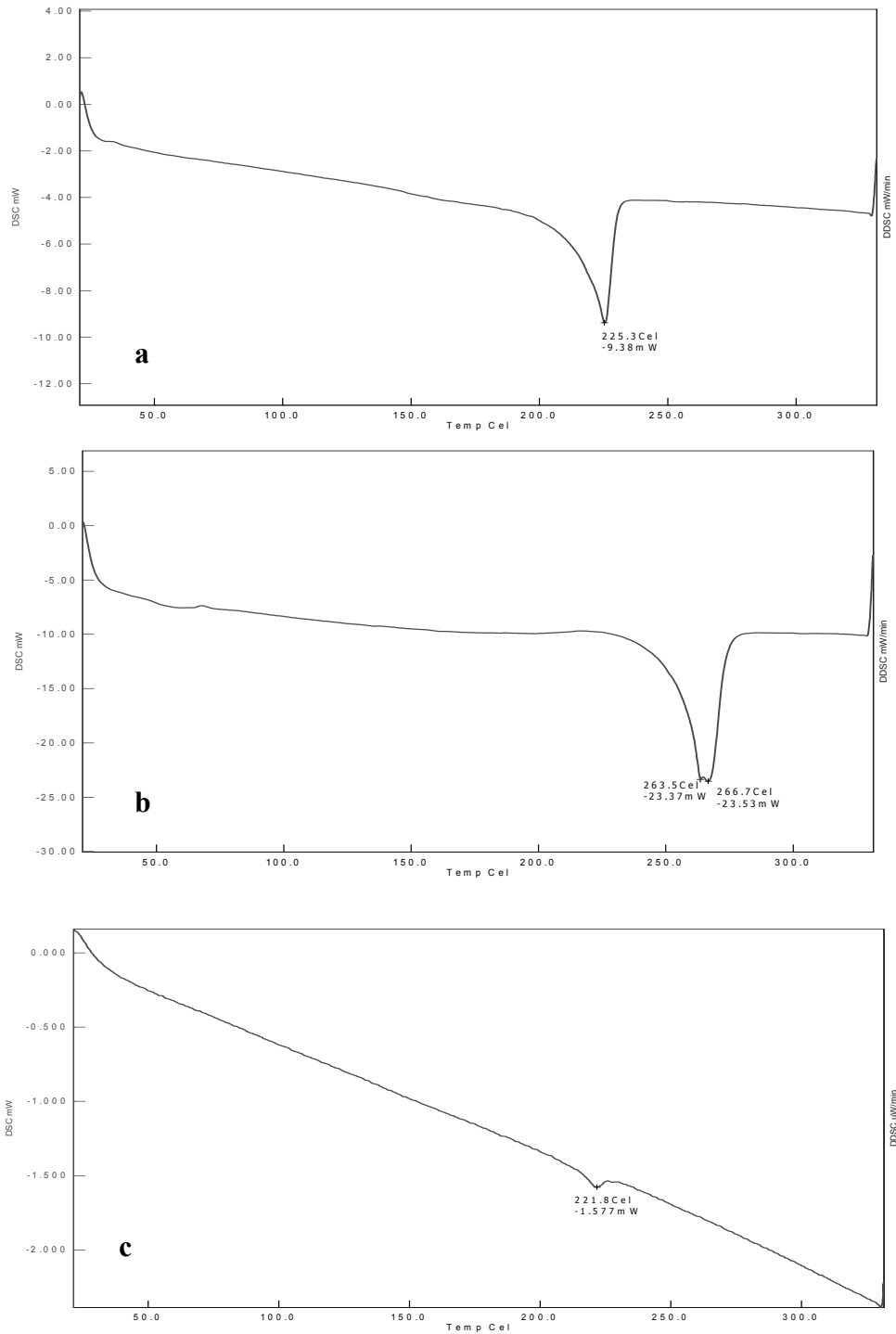


**Fig.6.** The DSC graphs of (a) PA 6, (b) PA 6.6 and (c) PA 4.6 pellets

When the DSC graphs of polyamide pellets in Figure 6 are examined in connection with the data given in Table 1, lack of glass transition temperature  $T_g$  in PA 4.6 pellet could be the result of highly crystalline polymer structure composed of possibly one homogenous type of crystalline region as

can be seen from single peak around 292°C. PA 6 and 6.6 pellets have twinning in their peaks in the melting regions due to a possible differentiating crystal structure showing a second but smaller melting peak near the main melting peak.

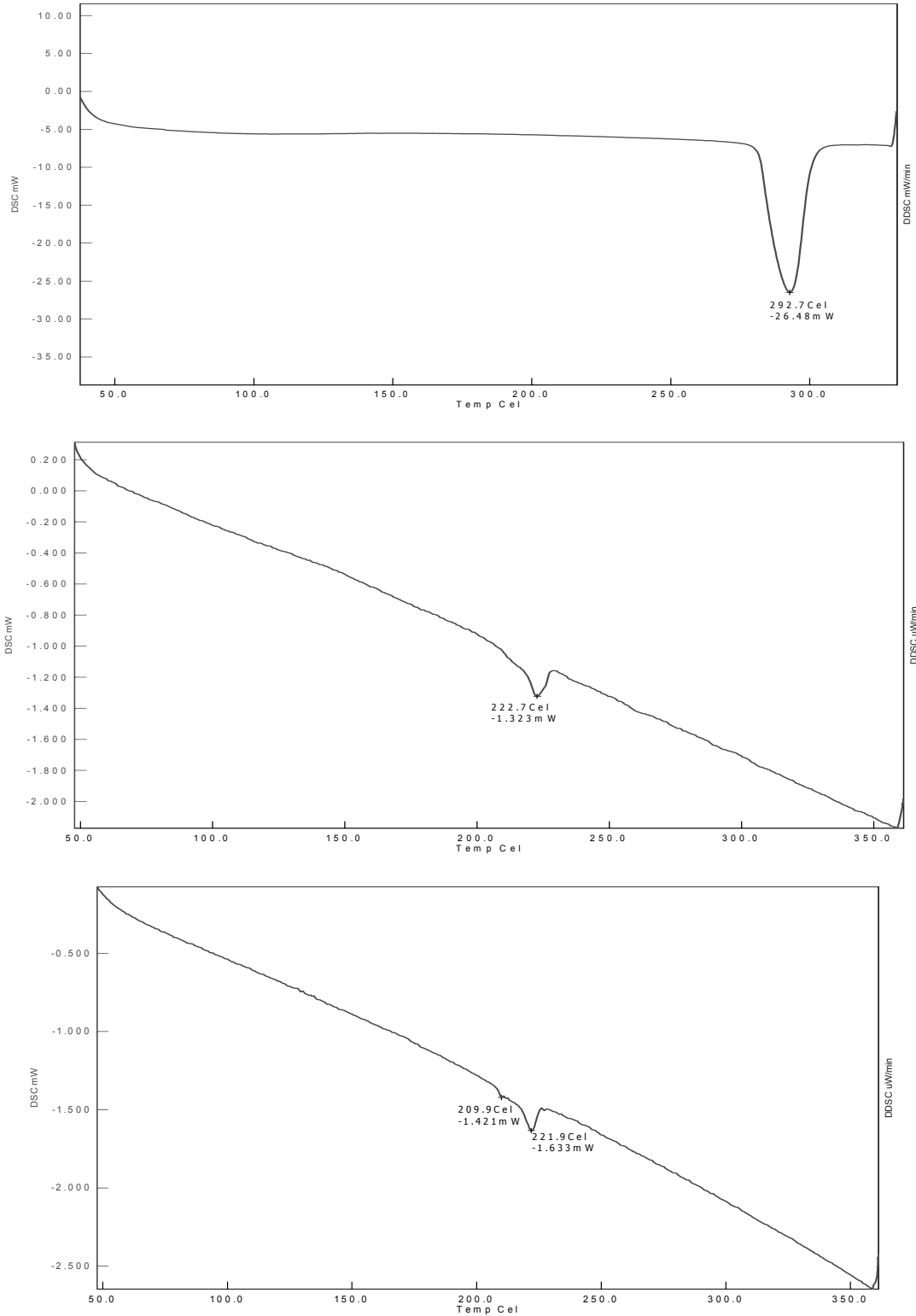


**Fig.7.** The DSC graphs of PA 6 nanofibers of (a) 13%, (b) 16% and (c) 20% conc.

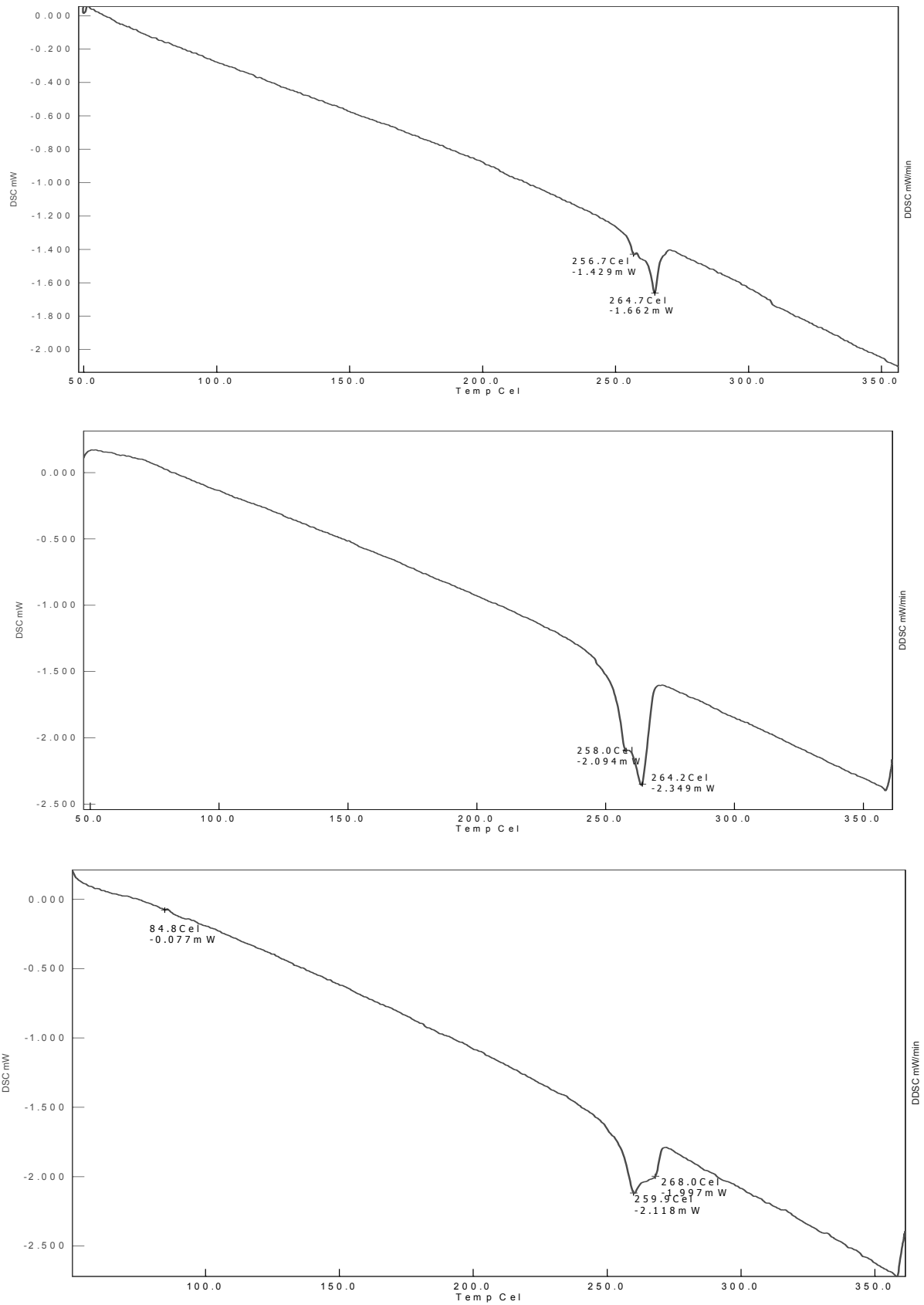


**Fig.8.** The DSC graphs of PA 6.6 nanofibers of (a) 13%, (b) 16% and (c) 20% conc.

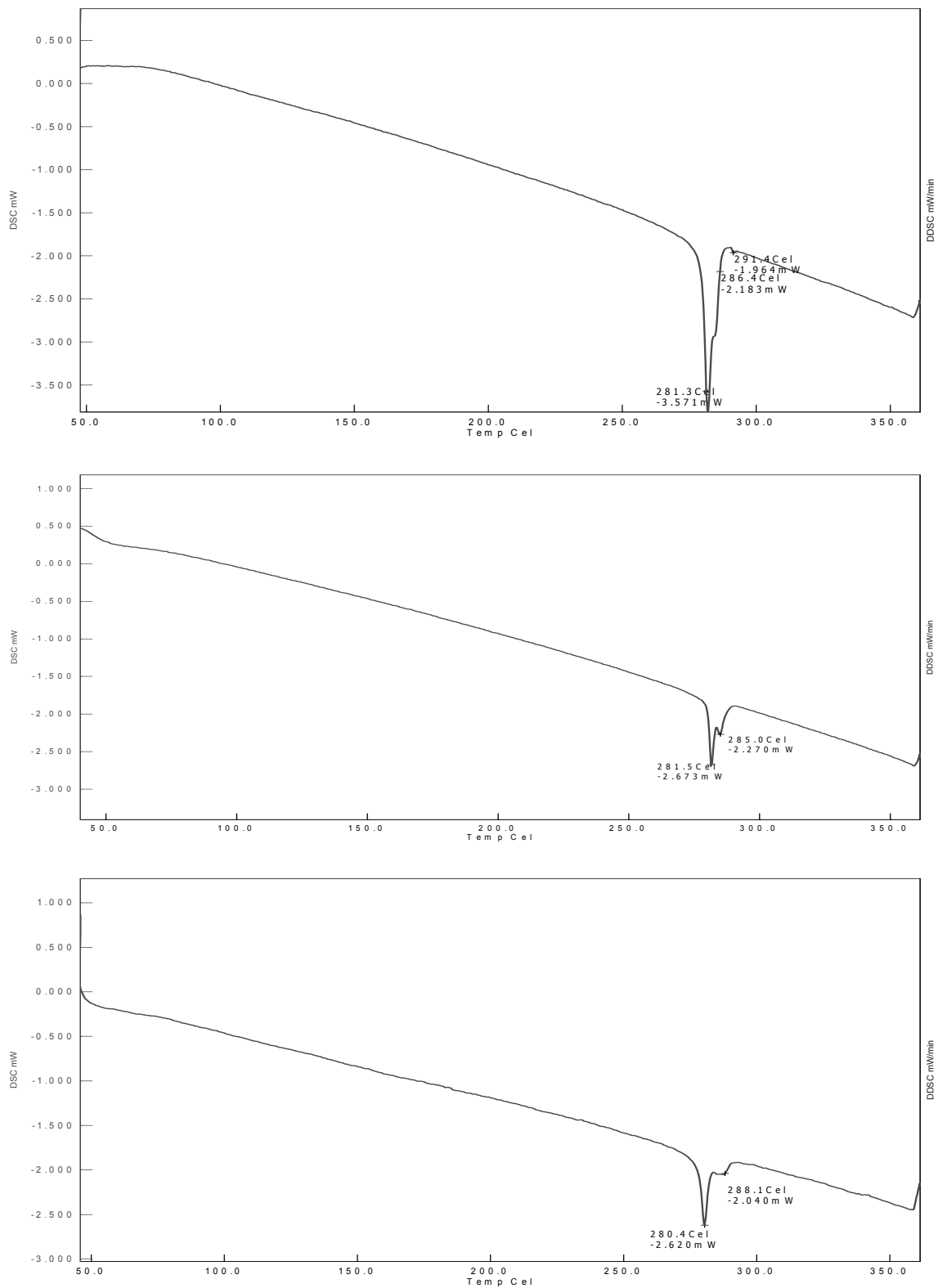


**Fig.9.** The DSC graphs of PA 4.6 nanofibers of (a) 13%, (b) 16% and (c) 20% conc.

DSC measurements of PA 6 (Figure 7), PA 6.6 (Figure 8) and PA 4.6 (Figure 9) showed that the melting temperature  $T_m$  increased as the crystallinity of polymer increased; PA 6 nanofibers generally had around 15% of crystallinity whereas PA 6.6 had around 25% and PA 4.6 had 65% (Table 5). PA 6 nanofibers showed quite homogeneous, one

type of crystalline region as could be seen from the one point, narrow melting peaks. PA 6.6 nanofibers, on the other hand, had two consecutive melting points in a broad melting area, possibly because of two types of different crystalline or well-oriented amorphous regions, which changed in ratio as the polymer concentration increased, as could be observed



from the dislocation of the lower  $T_m$ . The same phenomena occurred in PA 4.6, resulting twin peaks that did not exist in pellet form, but except that the bands showed a narrower band. Both PA 6.6 and PA 4.6 have similar polymer structures, but as it has a more symmetrical structure and greater amount of amide linkages, polyamide 4.6 showed higher melting temperature and ability to crystallize quicker than polyamide 6.6 in harmony with the data in literature (6). The crystallinity of pellets remained nearly the same (in PA 6.6) or decreased (in PA 6 and PA 4.6) when electrospun; this result is contrary to what is announced in Baji et al.'s study (7) which states that crystallinity increases after the electrospinning but is in parallel direction with the studies in

Ref. [13,14] stating a decrease in crystallinity after the electrospinning. The mechanism behind this may be that because of the short evaporation and solidification time in millisecond scale, structure formation has to happen fast. The nucleations of crystals should therefore be strongly quenched and the structure that results should be far from the equilibrium state. It has been reported that crystalline microstructure in electrospun fibers may not be well developed and that the crystal sizes may be quite small. The degree of crystallinity might be reduced and crystal modifications are expected to form high degree of imperfections (13).

**Table 5.** Mean crystallinity of polyamide nanofibrous surfaces

Polymer	Concentration (%)	$T_m$ (°C)	$\Delta H_f$ (J/g)	Crystallinity (%)
PA 6 ( $H_f=230$ J/g)*	13	222	16,5	7,17
	16	222	45,3	19,68
	20	222	31,2	13,57
PA 6.6 ( $H_f=226$ J/g)*	13	265	55,00	24,33
	16	264	63,3	28,00
	20	268	55,3	24,46
PA 4.6 ( $H_f=105$ J/g)*	13	285	72,1	68,66
	16	284	62,2	59,23
	20	287	64,7	61,61

\*:<http://www.tainstruments.com/pdf/literature/TN048.pdf>

**Table 6.** Tensile properties of polyamide nanofibrous surfaces

Polymer	Concentration (%)	Stress@peak (N/mm <sup>2</sup> )	Force@peak (N)	Strain@peak (%)	Young Modulus (N/mm <sup>2</sup> )	Surface thickness (mm)
PA 6	13	61,839	0,928	28,725	411,041	0,003
PA 6	16	31,064	0,466	20,267	310,387	0,003
PA 6	20	38,975	0,585	25,585	299,323	0,003
PA 6.6	13	40,788	0,816	18,384	429,522	0,004
PA 6.6	16	37,970	0,759	12,440	645,886	0,004
PA 6.6	20	25,672	0,385	30,248	278,363	0,003
PA 4.6	13	59,597	2,086	28,359	540,700	0,007
PA 4.6	16	37,200	0,558	29,422	311,935	0,003
PA 4.6	20	28,472	0,575	46,251	184,695	0,004

The mechanical properties of nanofibrous surfaces shown in Table 6 revealed that in all three polyamide types, the stress and strain at peak values as well as Young Modulus decreased as the concentration increased. In 20% concentration, the modulus of PA 4.6 was lower than PA 6 and PA 6.6, the result is in line with literature (8, 9). On the other hand it was vice versa for low concentration of 13%, where PA 4.6 had the highest modulus among the three polyamides. This may indicate that in low concentrations of PA 4.6, better orientated polymer chains and crystallinity, resulting in an increase in the tensile properties, could be obtained during electrospinning process.

## CONCLUSION

Three widely-used polyamides, PA 6, 6.6 and 4.6 were investigated for suitability in electrospinning and product

properties. PA 6 nanofibers below 100 nm could be electrospun and the smoothest nanofibers without beads could be produced from PA 4.6 in 13% concentration. Nanofiber diameters increased as the polymer concentration increased in all three polyamides. All nanofibrous surfaces were hydrophilic and had surface contact angles below 90°. The crystallinity of pellets dropped after electrospinning but yet PA 4.6 was the most crystalline amongst all nano surfaces. Tensile testing showed that the increase in polymer concentration in electrospinning solution effected the resulting modulus values adversely. PA 4.6 in low concentrations (as 13%) was found to give the best result in the most homogeneous fiber diameter and the biggest crystalline ratio in all three polyamide types.

---

## REFERENCES

1. Athira K.S., Pallab S., Kaushik C., 2014, "Fabrication of Poly(Caprolactone) Nanofibers by Electrospinning", *Journal of Polymer and Biopolymer Physics Chemistry*, Vol:2 (4), pp:62-66.
2. Bhardwaj N., Kundu S.C., 2010, "Electrospinning: A fascinating fiber fabrication technique", *Biotechnology Advances*, Vol:28, pp: 325–347.
3. Huang Z.M., Zhang Y.Z., Kotaki M., Ramakrishna S., 2003, "A review on polymer nanofibers by electrospinning and their applications in nanocomposites", *Composites Science and Technology*, Vol:63, pp: 2223-2253.
4. Adanur S., 1995, *Wellington Sears Handbook of Industrial Textiles*, ISBN 1-56676-340-1, pp:45.
5. Fried J.R., 2003, *Polymer Science and Technology, Second Edition*, ISBN 0-13-018168-4, pp:391.
6. Bunsell A.R., *Handbook of Tensile Properties of Textile and Technical Fibres*, 2009, The Textile Institute, Woodhead Publishing in Textiles: Number 91, Woodhead Publishing ISBN 978-1-84569-387-9, p.:211.
7. Baji A., Mai Y.W., Wong S.C., Abtahi M., Chen P., 2010, "Electrospinning of polymer nanofibers: Effects on oriented morphology, structures and tensile properties", *Composites Science and Technology*, Vol:70, pp: 703–718.
8. Schoenmaker B., Schueren L.V., Ceylan Ö., Clerck K., 2012, "Electrospun Polyamide 4.6 Nanofibrous Nonwovens: Parameter Study and Characterization", *Journal of Nanomaterials*, Article ID 860654, 9 pages.
9. Suzuki A., Endo A., 1997, "Preparation of high modulus nylon 46 fibres by high-temperature zone-drawing", *Polymer*, Vol:38, No:12, pp:3085-3089.
10. [http://web.mit.edu/5.32/www/Appendix\\_1\\_Qual\\_Instrumentation\\_03.pdf](http://web.mit.edu/5.32/www/Appendix_1_Qual_Instrumentation_03.pdf) (09.11.2016)
11. <http://chemistry.oregonstate.edu/courses/ch361-464/ch362/irinterp.htm> (09.11.2016)
12. Thompson C.J., Chase G.G., Yarin A.L., Reneker D.H., 2007, "Effects of parameters on nanofiber diameter determined from electrospinning model", *Polymer*, Vol: 48, pp:6913-6922.
13. Dersch R., Liu T., Schaper A. K., Greiner A., Wendorff J. H., 2003, "Electrospun Nanofibers: Internal Structure and Intrinsic Orientation", *Journal of Polymer Science: Part A: Polymer Chemistry*, Vol: 41, pp: 545–553.
14. Bergshoef M.M., Vancso G.J., 1999, "Transparent Nanocomposites with Ultrathin, Electrospun Nylon-4,6 Fiber Reinforcement", *Advanced Materials*, Vol: 11, No. 16, pp: 1362-1365.